



## Article

# Competitive Distribution of Public Goods: The Role of Quorum Sensing in the Development of Bacteria Colonies

Eleonora Alfinito <sup>1,\*</sup>  and Matteo Beccaria <sup>1,2,3</sup> 

<sup>1</sup> Department of Mathematics and Physics ‘Ennio De Giorgi’, University of Salento, I-73100 Lecce, Italy; matteo.beccaria@unisalento.it

<sup>2</sup> National Institute for Nuclear Physics (INFN) Sezione di Lecce, Via Arnesano, I-73100 Lecce, Italy

<sup>3</sup> National Biodiversity Future Center, I-90133 Palermo, Italy

\* Correspondence: eleonora.alfinito@unisalento.it

**Abstract:** The production of public goods is a necessary condition for the survival of the species, but it comes at the expense of individual growth. In a prototype bacterial colony, we model the role of quorum sensing as a resource redistribution mechanism. Two types of bacterial colonies are analyzed, one made up of a single strain and one made up of two different strains. Based on a recent series of experimental data present in the literature, we analyze two types of strains with different extinction times: strains that consume available resources very quickly, therefore becoming extinct quickly, and strains that consume resources slowly and die due to aging. We show that the proposed quorum sensing model describes the main experimental result that coexistence may favor the survival of both strains. Furthermore, the production of public goods is maximized when both types of individuals have the maximum proliferation output. Finally, we highlight the role played by so-called dormant cells in the duration of survival time. These cells are of particular interest because their ability to counteract different types of stress (e.g., the use of antibiotics) still constitutes a challenge.

**Keywords:** quorum sensing; cooperation; agent-based model



**Citation:** Alfinito, E.; Beccaria, M. Competitive Distribution of Public Goods: The Role of Quorum Sensing in the Development of Bacteria Colonies. *Biophysica* **2024**, *4*, 327–339. <https://doi.org/10.3390/biophysica4030023>

Academic Editors: Danilo Milardi and Javier Sancho

Received: 28 May 2024

Revised: 13 June 2024

Accepted: 19 June 2024

Published: 21 June 2024



**Copyright:** © 2024 by the authors. Licensee MDPI, Basel, Switzerland. This article is an open access article distributed under the terms and conditions of the Creative Commons Attribution (CC BY) license (<https://creativecommons.org/licenses/by/4.0/>).

## 1. Introduction

The development of bacterial colonies is a fascinating research topic where complexity of a well-organized system is implemented by the simplest biological elements, i.e., cells. Furthermore, understanding the mechanisms underlying colony growth has multiple interests because it can help in controlling and containing potentially dangerous strains [1,2] or conversely sustaining beneficial strains [3,4]. More generally, such mechanisms are useful for identifying common social mechanisms that can also be observed in multiple evolved species [5].

The available literature offers several models that describe social cooperation particularly between evolved beings. For instance, cooperation may be induced by forms of global awareness that achieve a higher level of well-being by reducing personal payoff and adopting risk-averse strategies [6–8].

In less evolved living beings, the concept of conscious awareness is presumably replaced by a sort of unconscious awareness associated with mechanisms of elementary communication performed through hormones, pheromones, or in general small molecules. This seems to be the basis of the functioning of very organized systems such as beehives, anthills, and again bacterial colonies.

In bacteria, this kind of communication is called *quorum sensing* (QS) [9,10]. It has a pivotal role in the production of both offspring and public goods like toxins, biofilm, bioluminescence, etc. Furthermore, in the framework of ecological competition, the concept of *competition-sensing* [11] was coined to describe abilities gained by bacteria in detecting and responding to ecological competition. In fact, one of these abilities is quorum sensing [11], which seems to be involved in the cooperative interaction of bacterial colonies [12–16].

The concept of awareness as well as other social characteristics such as that of cheater, defeater, and cooperator (which have a clear meaning in evolved species) lose their traditional meaning in the case of less evolved species where they may rather be related to different abilities in the management of nutrients (metabolism) or stressing conditions.

Generally speaking, it is not clear what are the conditions under which cooperation wins against individualism [17–20], but it is known that cooperation is widely adopted by living beings of different evolutive levels and has a key role in regulating ecological and also evolutionary processes [20]. Many proposed models of cooperation or mutualism produce results which appear to differ from real data [20], suggesting that some key element is still missing in our knowledge of this phenomenon.

Recent studies considered colonies of *Vibrio harveyi*, which is a bacterium widely diffused in aqueous environment and mainly known for its ability to produce bioluminescence. In this case, the role of QS in the maintenance of wellness in natural (wild-type) strains as well as its evolutive role in sustaining cooperation in bacteria colonies was highlighted [12–14]. Specifically, natural strains of this and probably other bacteria are supposed to be a well-mixed combination of strains classified as defectors/cooperators with respect to public goods (PG) production. It was observed that while defectors maximize their growth at the expense of PG production, cooperators do the opposite and maximize PG production at the expense of their growth. Both these strategies drive to extinction: in the former case due to exhaustion of resources, in the latter due to aging. While defeaters outcompete unconditional cooperator lineages, if mixed properly, QS may regulate the performance of both and produce a stable colony which is resilient against the attacks of enemies/defeaters [12].

In natural environments, bacteria compete mainly for space and nutrients [16,21] and metabolism plays a key role in ecological competition [11,21]. As expected, in conditions of a limited quantity of nutrients, competitors with high metabolism perform better than competitors with low metabolism. On the other hand, a more complex and partially unknown role is played by metabolism in conditions in which the quantity of nutrients changes (enrichment paradox) [22] or in describing the behavior of bacteria during dormancy [23].

In this paper, we outline a model where QS acts as a moderator between two strains characterized by two different social behaviors and promotes cooperation in agreement with experiments [12–14]. In particular, we model each strain as characterized by two specific biochemical mechanisms: the assimilation rate related to the metabolism of the cell [21] (higher metabolism, higher offspring production) and the productivity level of PG, i.e., the fraction of resources allocated for this purpose. Depending on the values of metabolism and productivity, we have four schematic characterizations of the single agent: (a) *cheater* with high metabolism and low productivity; (b) *defeater* with high metabolism and high productivity (it is defeated in offspring production due to the high quantity of resources driven to PG); (c) *cooperator* with low metabolism and high productivity; (d) *dormant* with low metabolism and low productivity. In our modeling, the limited quantity of resources (environmental conditions) and the existence of a maximal surviving time drive each of the categories to extinction in a short time. On the other hand, when suitably mixed, the two strains turn out to be able to perform better than both of the single ones in terms of survival time, fitness, and public goods production. The factor responsible for this interesting behavior is quorum sensing, here introduced as a long-range interaction among agents which acts as a moderator in the development of each type of agent. The model and results are detailed in the following sections.

## 2. Materials and Methods

We model a bacterial colony in a way that takes into account strains that display specific social behaviors [12–14]. If left to develop alone, they would produce extinction with little production of public goods. If properly mixed, they should exhibit a large PG production. The key element of the modeling is quorum sensing, previously introduced to

describe bioluminescence in *Vibrio harveyi* [24,25] and which is here shown to be able to provide some general benefits to the colony in agreement with experiments [12–14].

The model is intended to represent colonies of bacteria developing in a limited environment and limited food conditions in line with the description in [12–14]. The colonies are made up of single or multiple strains, each characterized by a specific rate of nutrient assimilation ( $\sigma$ ) and level of productivity ( $\alpha$ ) of public goods.

### Model

The proposed model is an agent-based model on a regular network [24–28]. The quantity of resources is limited. In the network, each node represents an occupiable position. Each node can be occupied by only one of two different types of agents, each identified by a productivity parameter  $\alpha$  which regulates the quantity of public goods produced and an assimilation rate  $\sigma$  that characterizes the agent type. The productivity parameter can be adjusted to achieve the best performance. A higher productivity reduces the offspring levels. Each kind of agent reproduces the features of a specific bacterial strain, and for this reason we will use the two terms interchangeably. Strains with a low assimilation rate (small  $\sigma$ ) reproduce with difficulty and finally die out due to aging. On the other hand, strains with a high assimilation rate reproduce easily and quickly deplete the environmental resources, thus dying due to hunger. Strains that adopt low productive behavior (small  $\alpha$ ) are most effective in producing offspring, and the opposite happens for strains that adopt highly productive behavior.

The model implements the concept of *quorum sensing* (QS), i.e., a long-range interaction between cells, via an effective long-range potential instead of physical exchange of small molecules (autoinducers [9,10]). This potential is produced by a characteristic of the cell, i.e., the *sensing-charge* ( $Q$ ), which represents the strength of the cell/agent and can be associated with its size. The value of  $Q$  here takes integer values and has multiple roles. It determines whether the agent can reproduce by donating half of  $Q$  to the offspring. It also determines the quantity of energy (nutrients) that each agent can receive. It selects the node that the offspring can occupy and, finally, determines the quantity of public goods produced by the colony.

The evolution of each agent stops when it reaches the maximum value of  $Q_{\max}$ . On the other hand, the energy necessary to improve the *sensing-charge* is ideally taken from outside, i.e., from the environment, and there is a maximum amount of energy that the colony may receive. When this threshold is reached, the colony evolution stops. Each agent also has an age indicator which brings the *sensing-charge* value to zero once a maximum value  $\tau$  is reached, whereupon no agent is present on that node.

The colony is allowed to evolve for subsequent iterations, and the assumed configuration is stored at each iteration. The age indicator grows by one unit at each step if the *sensing-charge* value does not change.

The initial value of  $Q$  (0/1) is assigned stochastically in the first iteration in order to distribute a quantity of *sensing-charges* equal to an assigned fraction of the total quantity of nodes.

At each iteration, each agent receives energy which it uses for reproduction or migration in proportion to its assimilation rate. The amount of received energy depends on the energy distributed in the colony. In turn, this depends on the existing *sensing-charges* and on its own productivity and increases as the aptitude for productivity decreases. The final quantity of nutrients used by each agent depends on its own assimilation rate.

Finally, the colony produces public goods (nutrients, viral agents, bioluminescence, etc. [9,10]) which are a product of QS and specifically of the level of cooperativity [24,25].

In our model, links and nodes give complementary information about the colony. Specifically, while the colony growth depends on the nodes of the network, the production of PG is described by means of the links by solving a random resistor network (RRN) [29] that overlays the grid and evolves with it. The impedance of this RRN depends on the amount and distribution of *sensing-charges* in the network and converts these data into

a measurable quantity that we identify with the specific public goods produced by the colony, for example bioluminescence [24].

The procedure is detailed as follows and is resumed in the flow chart reported in Figure 1:

1. LANDSCAPE INITIALIZATION

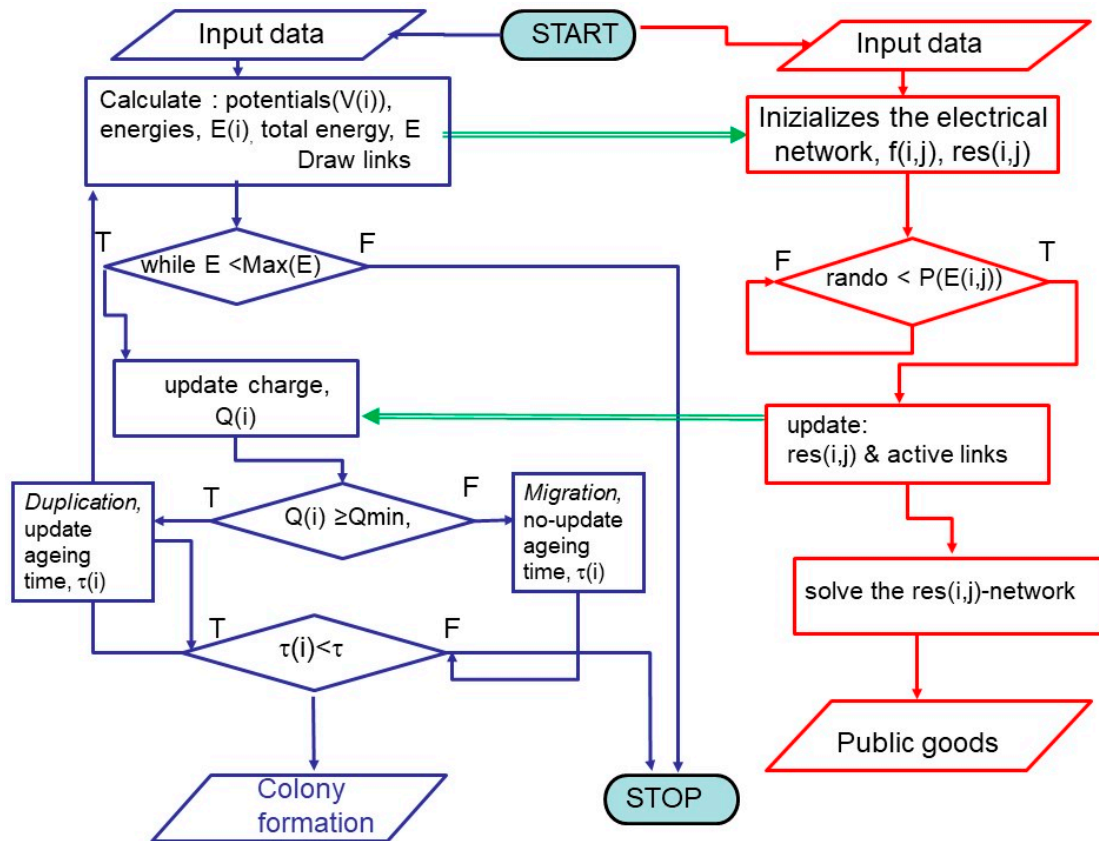


Figure 1. Flow chart of the algorithm described in Section 2.

INPUT DATA input data (shown in Table 1) include a random distribution of agents with  $Q = 1$  in the grid, in agreement with the chosen fraction of occupiable sites. Each node may be occupied by only a single-type agent.

Table 1. Model parameters. We briefly recall their meaning and the values adopted in simulations.

$L_x, L_y$	Dimensions of the rectangular grid	$20 \times 20$
$f_0$	Initial fraction of occupied nodes	0.1
$\alpha$	Productivity coefficient	$[10^{-4}-10]$
$r_{max}, r_{min}$	Resistance values entering the link resistance formula	$r_{max}= 1000, r_{min}= 1(a.u.)$
$g$	Parameter in the Hill-like function, controlling the resistance interpolation	0.01
$\sigma$	Assimilation rate	$[1-30]$
$Q_{max}$	Maximum value of the activity triggering death or biofilm formation	80
$\tau$	Ageing time	10 (a.u.)
$Max(E)$	Maximal fraction of energy to be used	0.9
$Q_{min}$	Minimal reproduction size	2

POTENTIAL DESIGNATION the potential  $V$  of each node and the energy of the whole network are computed. For the  $l$ -th node, the potential  $V(l)$  and its energy  $\varepsilon(l)$  are given by

$$V(l) = \sum_{j \neq l}^N \frac{Q(j)}{Dist(j,l)}, \quad \varepsilon(l) = Q(l) \sum_{j \neq l}^N \frac{Q(j)}{Dist(j,l)}, \quad (1)$$

where  $N = L_x \times L_y$  is the network size and  $Dist(j,l)$  is the Euclidean distance between the two nodes  $l$  and  $j$ .  $Q(k)$  is the *sensing-charge* of the  $k$ -agent independently on its type.

The energy of the network is computed as

$$Energy = \frac{1}{2} \sum_{\substack{i,j=1 \\ (i \neq j)}}^N \frac{Q(i)Q(j)}{Dist(i,j)} \quad (2)$$

When  $Energy \geq Max(E)$  the evolution stops.

NETWORK SETUP Each agent explores the other agents in the grid and opens links with the ones with lower potential. The matrix of links is thus nonsymmetric.

## 2. RRN INIZIALIZATION

RESISTANCE NETWORK the link between the nodes  $n, m$  is equipped with an elementary resistance:  $res(n, m) = r_{max} Dist(n, m)$ , where  $r_{max}$  is an asymptotically large resistivity value. Unlike the matrix of links, the matrix  $res(n, m)$  is symmetric.

Finally, following a strategy formerly used in the description of the electric performances of biological matter [30–32], a pair of ideal extended electrical contacts is attached to the ends of the network and ideally connected with a low DC bias [30,31].

## 3. COLONY EVOLUTION

LINK ACTIVATION Each link across the  $n, m$  nodes is *activated* with the following probability:

$$p(n, m) = \min(1, \exp(-\alpha^3 \Delta E_{n,m})), \quad \Delta E_{n,m} = \frac{\varepsilon(n) - \varepsilon(m)}{Energy} \quad (3)$$

The parameter  $\alpha$  is the cooperativity coefficient, and  $Energy$  (see Equation (2)) measures the quantity of *sensing-charges* present in the landscape. Only the activated links play a role in the production of public goods production and offspring.

The specific expression of the probability of activation in Equation (3) accounts for different aspects, i.e.,

1. the amount of energy distributed in the landscape, being larger for larger energy, thus producing an autocatalytic effect;
2. the difference in energy between the considered agents, being larger for smaller differences, thus allowing a better distribution of activated links among nodes similar in energy;
3. the productivity of the agent, which represents the canalization of resources, in offspring or public goods production, thus producing less active links for higher productivity.

PUBLIC GOODS PRODUCTION If a link has been activated, then its resistance decreases according to the following law:

$$res(n, m) = Dist(n, m)[r_{max}(1 - f(n, m)) + r_{min}f(n, m)], \quad (4)$$

where  $r_{min}$  is the minimal value assigned to the resistivity and the interpolating function  $f(n, m)$  is taken to have a Hill-like shape [33,34]:

$$f(n, m) = \frac{w^\gamma(n, m)}{K^\gamma + w^\gamma(n, m)}, \quad (5)$$



with  $w(n, m)$  the mean value of the *sensing-charges* of the nodes  $n, m$ . The Hill number  $\gamma$  coincides with the productivity coefficient for a single strain. For the case of two strains, it is given by their mean value,  $\langle \alpha \rangle$ . Notice that in Equation (5)  $\gamma$  is the colony cooperativity index, which we related in [25] to the amount of bioluminescence produced by several mutants of *Vibrio harveyi*. As a matter of fact, it represents the strength with which the agents present in the network cooperate in the formation of the public goods to the extent of their *sensing-charges*. The parameter  $K = gQ_{max}$  controls the steepness of the interpolation and hence the quantity of *sensing-charges* necessary to reach the minimal resistance.

**OFFSPRING PRODUCTION** Each agent receives energy from other nodes with a higher potential. In particular, the *sensing-charge* value grows as

$$Q(n) \rightarrow Q(n) + \text{floor}\left(\frac{\sigma * \text{links}(n)}{N}\right), \quad (6)$$

where  $1 < \sigma < N$  is the assimilation rate specific to the considered agent and  $\text{links}(n)$  is the number of links activated and connected to the  $n$ -th node.

In this step for each agent, we consider migration/duplication transitions. An empty site is selected for reproduction. The choice is made by first sorting the neighbors in order of increasing potential. Then the  $k$ -th node in the list is selected with probability [24,25]

$$p(k) = \frac{(k-1)!}{9^{k-1}} \left(1 - \frac{k}{9}\right), \quad k = 1, \dots, 8. \quad (7)$$

This formula corresponds to choosing the minimum potential node ( $k = 1$ ) with probability  $(1-1/9)$ , and otherwise with probability  $1/9$  choosing the second ( $k = 2$ ) with probability  $(1-2/9)$ , and so on. It is possible that none of the 8 nodes is chosen, although this happens with the very small probability  $(8!/9^8) = 0.00093$ .

If the parent agent has the minimum nonzero value  $Q = 1$ , it will migrate to the target node, which inherits  $Q = 1$  while the parent node is set to  $Q = 0$ .

If instead the parent node has  $Q \geq 2$ , it gives half of its *sensing-charge* to the target node, thus implementing a binary-fission event [24,25]. Parent and offspring have the same assimilation rate and cooperative coefficient.

The final extinction of the colony happens due to greed or starvation, the former occurring when the agents have consumed all the available resources, the latter when the agents have not been able to obtain energy and die due to aging.

The overall free parameters of our simulations are listed in the following Table 1 (in the third column we report the fixed values used in the presented simulations).

To give an idea of the typical model runtime, we ran 60 statistical realizations on an Intel Xeon workstation in about one hour. The available multiple processors were exploited to explore in parallel different parameter sets.

### 3. Results

Our analysis aims to detect the conditions under which cohabitation performs better than living alone, looking in particular at fitness, i.e., the ability to spread in the landscape. Fitness is here measured by the ratio  $f = \frac{N_f}{N_i}$ , where for each competitor  $N_{f/i}$  is the final/initial number of agents and colony survival time is given in terms of iteration steps.

Simulations were performed on grids of size  $20 \times 20$  and averaged over 30 repetitions of the stochastic evolution.

We considered two situations corresponding to a single strain or two-strain colonies.

#### 3.1. Single-Strain Colonies (SSC): Investigation on the Conditions for Reproduction

Different strains with an assimilation rate ( $\sigma$ ) between 1 and 30 were evolved using different productivity levels ( $\alpha$ ). For  $\sigma < 9$ , no-growing (NG) is the permanent condition of the strains (also exploring very small values of  $\alpha$ , here not reported). They all die due to aging (dormant cells). On the other hand, at the high value  $\sigma = 30$  only the highest

productivity level ( $\alpha = 10$ ) produces NG, and no death due to aging is observed as long as  $\alpha$  is less than 5. The colony quickly consumes the available nutrients and dies out. At intermediate values of  $\alpha$ , the probability of NG depends on  $\alpha$  and  $\sigma$  (see Figure 2). Extinction due to either aging or resource exhaustion may occur. Figure 2 reports the % of realizations in which extinction is due to aging instead of resource exhaustion. The initial concentration of agents is 10% of occupiable sites.

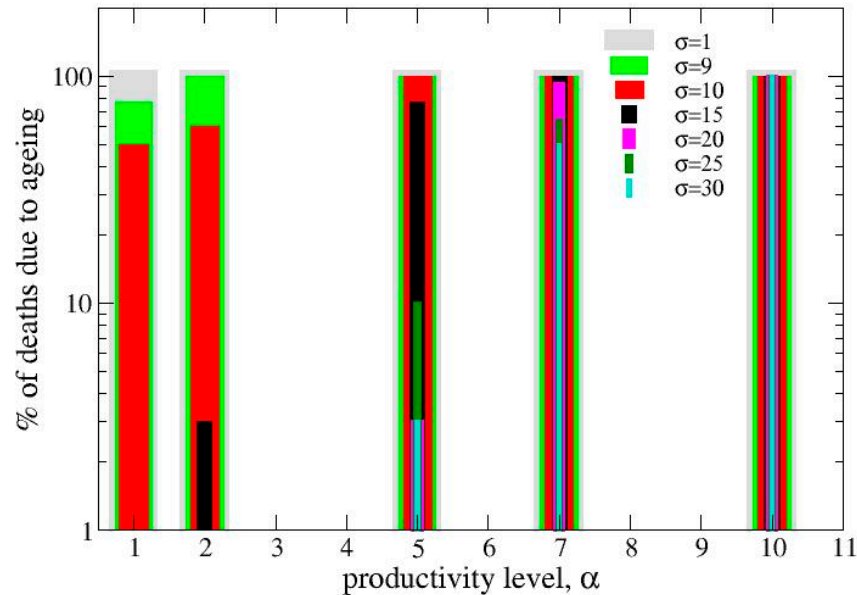


**Figure 2.** Percentage of colonies died due to ageing in single-strain colony evolutions. Data correspond to strains with different values of the assimilation rate ( $\sigma$ ) from 1 to 30 evaluated in the range of productivity ( $\alpha$ ) from 1 to 10. Stochastic averaging is over 30 realizations. Grid size is  $20 \times 20$  and the initial percentage of seeds is 10%.

### 3.2. Two-Strain Colonies

The first investigation concerns the comparison between a (strong) cooperators ( $\sigma = 2$ ,  $\alpha_1 = 10$ ) and a cheater ( $\sigma = 20$ ,  $\alpha_2 = 0.1$ ). The former has quite long life (20 time-units) and dies due to aging, while the latter has short life (13 time units) and dies from nutrient depletion. The cooperators has a production of PG about 4-fold larger than that of the cheater, although quite small (0.3 a.u.). When they are mixed in equal percentages, the resulting colony shows a survival time approximately as long as that of the cooperators (Figures 3 and 4) and a huge PG production (Figure 5,  $\gamma = \langle \alpha \rangle = 5.05$ ). The dynamic of colony development is shown in Figure 3 for cheaters alone (a), cooperators alone (c), and the mixed combination (b). Notice that in the single state, cooperators do not reproduce and migrate until extinction. The extinction event is not reported in Figure 3c. As a final remark, we can notice that the agents tend to fill the boundaries before other sites: This is due to the choice of privileging positions with the lowest potential, in agreement with Equation (7).

Finally, we have investigated the colony performance using a low-metabolism strain, nonprolific at the lowest values of  $\alpha$ , (a dormant strain), hereafter named **L**, and a high-metabolism strain, nonprolific for  $\alpha > 5$ , hereafter named **H**. They were mixed at an equal initial concentration (5%), named **Mix**, and the performances were recorded in terms of survival time and fitness. The selected assimilation rates are  $\sigma = 2$ , 20, respectively, and the cooperative level of the high-performing strain  $\alpha_2$  varies in the range  $[10^{-4}-10]$ . These values of  $\alpha_2$  describe social behaviors going from cheaters to defeater, while the productivity level of the low-performing strain  $\alpha_1$  is taken equal 2.

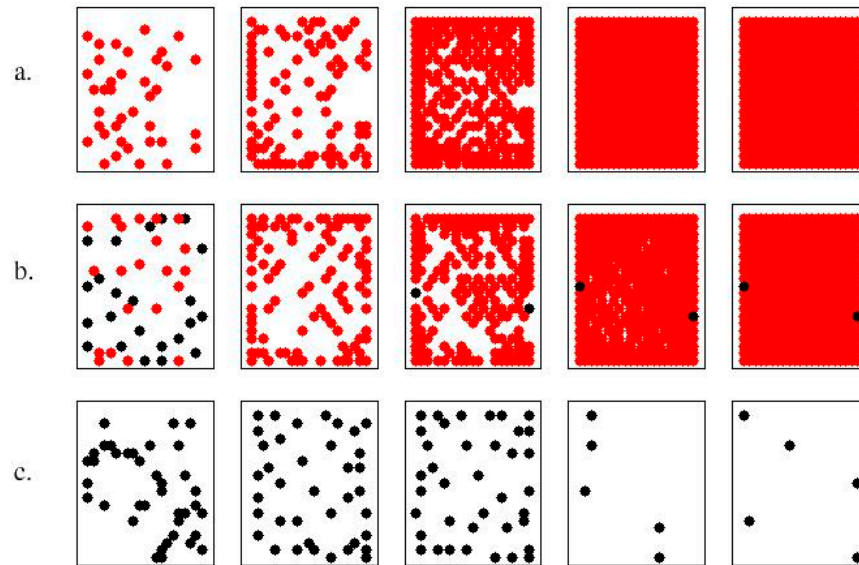


**Figure 3.** Time evolution of pure and complex state. Data concerns: (a) a pure state of high-metabolism agents, **H**, (red); (c) a pure-state of low-metabolism agents, **L**, (black); (b) the mixed state of both in the initial percentages of 10%, 10% and (5%+5%), respectively (red for **H**, black for **L**). The assimilation rates ( $\sigma$ ) are 2,20, for **L** and **H**, respectively, and the productivity values ( $\alpha$ ) are 10,01 for **L** and **H**, respectively. Initial and final configurations are reported for each kind of colony. Last iteration is 13 for row (a), 22 for row (b), 20 for row (c).

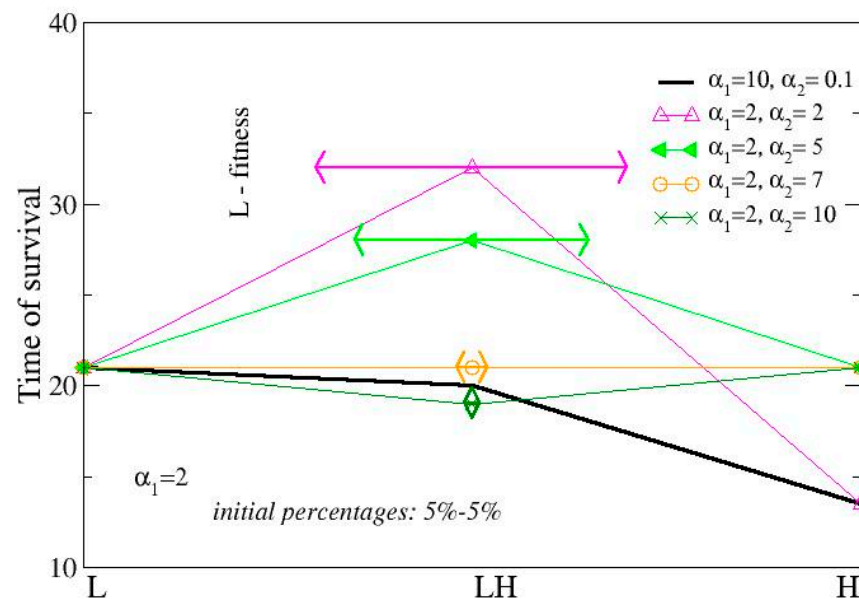


**Figure 4.** Survival times of mixed states. Data concerns: single-strain colonies of low-metabolism cells ( $\sigma_1 = 2$ ) (**L**); single-strain colonies of high-metabolism cells, ( $\sigma_2 = 20$ ) (**H**); mixed states of both (**LH**). The initial percentages are 10% for the single-strain colonies and 5% + 5%, for the mixed state. Horizontal lines report the fitness of the **L** in the mixed state, which goes from 1.6 for  $\alpha_2 \leq 1$  to 0 for  $\alpha_2 = 5$ . Black bold line describes the colony evolution of a strong cooperator ( $\sigma_1 = 2$ ,  $\alpha_1 = 10$ ) and a cheater ( $\sigma_2 = 20$ ,  $\alpha_2 = 0.1$ ). Time is calculated in iteration steps.

The lifetime of the **L** strain is determined only by the maximal aging time ( $\tau$ ) and can be made as long as desired. Each iteration corresponds to a time step. The survival time of the **H** strain at low values of the productivity value is quite a bit smaller than that of the **L** strain because it rapidly multiplies while consuming the available resources. The smaller the quantity of available resources, the smaller the lifetime. When the productivity rate



grows, the probability of becoming nonprolific increases and the lifetime tends to that of the L strain.

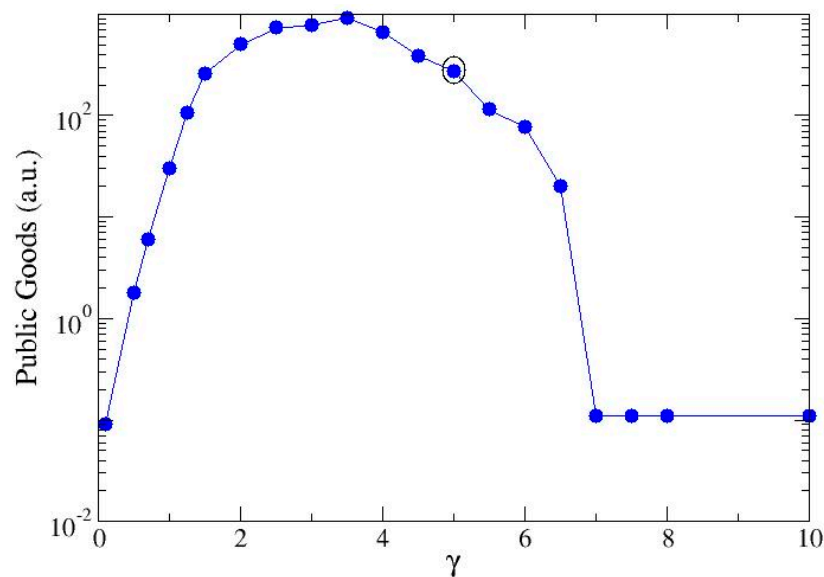


**Figure 5.** Public goods produced by a mixed colony calculated for different values of the cooperativity value  $\gamma$ , here calculated as the mean value between the two productivity values  $\langle\alpha\rangle$ . Both strains have the same value of the cooperativity value given by the average of the single strain cooperativity coefficient. The quantity of public goods is here measured in terms of the current that flows inside the network. Each point is the mean value over a set of 30 realizations. The black circle highlights the value  $\langle\alpha\rangle = 5.05$ : it refers to the mixed state of a cheater ( $\sigma = 20$ ,  $\alpha = 0.1$ ) and a strong cooperator ( $\sigma = 2$ ,  $\alpha = 10$ ) previously described in Figure 3c.

For  $\alpha_2$  smaller than five, the mixed state **Mix** guarantees a better outcome than the low-performing strain. It changes from sterile to low prolific (fitness larger than 1) and extends the survival times of both strains compared to the single states. For a very high cooperative level ( $\alpha_2 > 5$ ), both the high- and low-performing strains become even less and less prolific. The landscape is initially invaded by the high-performing strain, and later it too becomes extinct.

This behavior is due to the long-range interaction, i.e., to QS that distributes the *sensing-charges* to the extent that they are present in the landscape and without distinguishing what they are produced by. Thus, the sterile strain receives many more *sensing-charges* than it would receive in a landscape populated only by sterile cells. The fertile strain receives instead fewer *sensing-charges* than in a landscape populated only by fertile cells. In this way, the sterile ones can reproduce and do not die from aging. Also, fertile cells do not consume resources too quickly. The fitness of sterile cells is greater than zero, and the overall survival time is lengthened because the resources are consumed less quickly.

The survival time of mixed states with  $\alpha_1 = 2$  and  $\alpha_2$  varying from  $10^{-4}$  to 2 roughly doubles the value of the **H** strain, and the fitness of **L** is 1.6 and is quite insensitive of the value of  $\alpha_2$ . For larger values of  $\alpha_2$ , the fitness of **L** decreases until zero (at  $\alpha_2 \geq 7$ ). Only a small fraction of **H** does not die due to aging, and the survival time of the mixed state **Mix** tends to the survival time of **L**. For higher values of  $\alpha_2$ , both **L** and **H** are nonprolific, and the survival time of the mixed state is smaller than that of single state due to the smaller initial concentration.

For the selected pair of strains ( $\sigma = 2, 20$ ), the production of public goods depends on the value of the Hill number  $\gamma$ , here assumed equal to the mean of the productivity rates  $\langle\alpha\rangle$  (see Equation (5)). It has an initial growth, followed by a decrease due to the reduced ability of the strains to reproduce (Figure 5). In the present analysis, the maximum has been reached for  $\langle\alpha\rangle$  close to 3.5. Larger values of  $\langle\alpha\rangle$  no longer allow the strains to reciprocally

sustain themselves, and the most proficient strain invades the landscape. Furthermore, the minimal values are related to two different conditions: a. low cooperativity, i.e., small quantities of resources are directed towards the production of PG and, instead, used for offspring, and b. high cooperativity, i.e., the maximum quantity of resources is allocated to the production of PG, but the surviving agents are few and the final result is of scarce production.

In Figure 6, we show the time evolution of a seed composed of: (a) 10% of an L strain ( $\alpha_1 = 2$ ) and (b) 5% + 5% of L and H strains. The red dots are for the H strain ( $\alpha_2 = 10^{-4}$ ), and the black dots are for the L strain. We can observe that while the L strain dies out in a few (15) steps, it survives and reproduces in the mixed state, reaching a fitness value of 1.6. Survival time is doubled with respect to the evolution of the single strain.

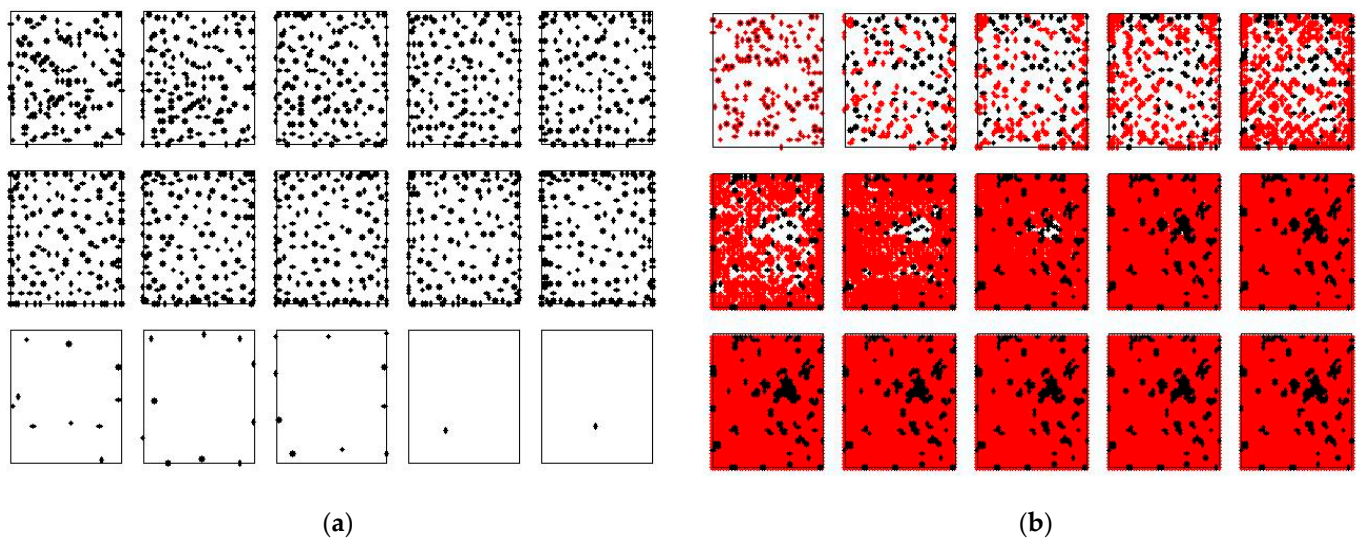


**Figure 6.** Time evolution of the L single state (a) and the Mix mixed state (b). The initial concentration of active nodes is 10%. The productivity rate  $\sigma$  is 2 for the L strain and  $10^{-4}$  for the H strain. The maximal aging time  $\tau$  is 10 (see Table 1). Last iteration is 15 for L and 32 for Mix. Black dots are for L, while red dots are for H.

#### 4. Discussion

The relevance of quorum sensing (QS) in the regulation of biological activity of bacteria colonies is well known [9,10]. Many models are formulated to describe its effects, based on deterministic equations [35–37] as well as stochastic simulations [38–41]. On the other hand, the precise role of QS in other kinds of regulatory mechanisms, like those underlying ecological competition, has been sketched although not clarified [11–15,17].

In previous studies, we proposed a model of QS described as a long-range interaction between bacteria represented as a collection of agents living on a regular grid and coupled by Coulomb-like interaction. The associated complex network is dynamical and self-generated. It grows as the number of agents increases and new mutual connections are established. Following previous studies, the network growth is monitored by means of an ideal flux of current whose intensity corresponds to some kind of public goods (PG), specifically bioluminescence, produced by the colony [24,25].

In the present investigation we are interested in a scenario of ecological competition (exploitative competition) between strains differing in the metabolism (assimilation rate) and productivity levels. The individual agents show a specific social behavior when single strain colonies (SSC) are considered. Remarkably, their social traits may change when several strains are simultaneously present and are in mutual metabolic competition.

This may be regarded as an instance of exploitative competition among species, i.e., a competition without direct interference, but instead indirectly triggered due to mutual subtraction of nutrients [11,21].

In our analysis, we focused on a colony made of two competitors comparing the performance of the mixed system with that of SSC. As we mentioned above, the two strains are characterized by different metabolic rates, and we examined the dependence on the productivity rate of the strain with higher metabolism (**H**). The considered productivity levels correspond to social behavior interpolating from single species colony SSC-cheater to SSC-defeater. Instead, the species with lower metabolism (**L**) is classified as an SSC-dormant and remains unchanged throughout the analysis.

Cooperation is here meant as the overall propensity of the colony to produce public goods. Each strain has a specific ability in producing these benefits, and this may be modified in the presence of a second, different strain. When this brings an advantage to the colony, we have cooperation; otherwise, we have anti-cooperation. The cooperative character of agents is quantified in terms of a cooperative index  $\gamma = \langle \alpha \rangle$  (Equation (5)) calculated as the mean value of the productivities of the two single strains. The amount of produced PG grows with  $\gamma$  in the region of cooperation and decreases with  $\gamma$  in the region of anti-cooperation (Figure 5). In the colony evolution, both the present (competing) strains attain  $\gamma$  as the productivity index. In this sense, quorum sensing acts as a mediator between different kinds of competitors.

As long as **H** has a productivity index low enough to be classified as an SSC-cheater, the cooperativity index is also low. In this situation, **L** becomes able to compete with **H** because it may exploit the greater available quantity of local resources (compared to that produced by itself). On the other hand, it also happens that **H** slows down its development due to the reduced quantity of local resources (compared to the SSC case). As a consequence, the coexistence of both species leads (with different fitness) to a colony survival time larger than that of a single strain, and the amount of produced PG is high, showing cooperation.

A completely different scenario is observed when the strain **H** has a high productivity value larger than 5. In this case, the **H** species changes its social trait from SSC-cheater to SSC-defeater. This happens because in the development of an SSC, the quantity of offspring produced is low and therefore the amount of PG is also small. On the other hand, since the common (averaged) value of cooperation increases, the **L** species becomes incapable of reproducing. Therefore, **H** completely outperforms **L**, and both the quantity of PG and colony survival time decrease. In this case, there is anti-cooperation. By further increasing the productivity of the SSC-defeater **H**, it also becomes incapable of reproducing, and the produced PG goes to zero. The survival time is the characteristic one of the SSD-dormant. This kind of outcome resembles the so-called “tragedy of commons” described in [15] as an effect of an increased cost of cooperation in a mixed colony.

From the above discussion emerges the key role of our choice of representing the interaction between coexisting strains assuming a common cooperative index equal to the mean value of the productivity levels of the single strains. This feature attempts to implement in a straightforward way the observation that quorum sensing operates mediating the features of the concurring strains [12–14,21]. The advantages for the colony in terms of fitness, survival time, and total PG production are a consequence of this choice. Such improved behaviors are detectable also in the case of equal values of productivity, in strains with different assimilation rates.

In conclusion, we showed that a QS mechanism described by a long-range interaction between bacterial cells is able to regulate cell growth and to stabilize cooperation between strains with different social behaviors. In particular, we analyzed the interaction between a strain of non-growing cells (dormant) and high-growing cells with variable productivity levels. We observed that they can profitably coexist until the high-metabolism species is not required to produce too much PG. The cooperation mechanism works in scenarios where the sub-population of slowly growing dormant cells sustains the fast-growing cells and has a key role in the persistence of the latter. This could help explaining the resurgence of some infections when treated with antibiotics that do not attack dormant cells [23].

**Author Contributions:** Both the authors contributed equally to this study. Conceptualization, E.A.; validation, E.A. and M.B.; writing—original draft preparation, E.A.; writing—review and editing, M.B. All authors have read and agreed to the published version of the manuscript.

**Funding:** This study received no external funding.

**Data Availability Statement:** Data and code will be made available on reasonable request.

**Conflicts of Interest:** The authors declare no conflicts of interest.

## References

1. Tang, K.; Zang, X.-H. Quorum quenching agents: Resources for antivirulence therapy. *Mar. Drugs* **2014**, *12*, 3245–3282. [[CrossRef](#)]
2. Appelbaum, P.C. 2012 and beyond: Potential for the start of a second pre-antibiotic era? *J. Antimicrob. Chemother.* **2012**, *67*, 2062–2068. [[CrossRef](#)] [[PubMed](#)]
3. Nguyen, T.H.; Goycoolea, F.M. Chitosan/Cyclodextrin/TPP nanoparticles loaded with quercetin as novel bacterial quorum sensing inhibitors. *Molecules* **2017**, *22*, 1975. [[CrossRef](#)]
4. Nguyen, H.T.; Hensel, A.; Goycoolea, F.M. Chitosan/cyclodextrin surface-adsorbed naringenin-loaded nanocapsules enhance bacterial quorum quenching and anti-biofilm activities. *Colloids Surf. B Biointerfaces* **2022**, *211*, 112281. [[CrossRef](#)]
5. Alfinito, E.; Barra, A.; Beccaria, M.; Fachechi, A.; Macorini, G. An evolutionary game model for behavioral gambit of loyalists: Global awareness and risk-aversion. *Europhys. Lett.* **2018**, *121*, 38001. [[CrossRef](#)]
6. Smith, J.M. The theory of games and the evolution of animal conflicts. *J. Theor. Biol.* **1974**, *47*, 209–221. [[CrossRef](#)]
7. Weibull, J.W. *Evolutionary Game Theory*; MIT Press: Cambridge, MA, USA, 1997.
8. Parsek, M.R.; Greenberg, E.P. Sociomicrobiology: The connections between quorum sensing and biofilms. *Trends Microbiol.* **2005**, *13*, 27–33. [[CrossRef](#)]
9. Henke, J.M.; Bassler, B.L. Three parallel quorum-sensing systems regulate gene expression in *Vibrio harveyi*. *J. Bacteriol.* **2004**, *186*, 6902–6914. [[CrossRef](#)] [[PubMed](#)]
10. Miller, M.B.; Bassler, B.L. Quorum sensing in bacteria. *Annu. Rev. Microbiol.* **2001**, *55*, 165–199. [[CrossRef](#)]
11. Cornforth, D.M.; Foster, K.R. Competition sensing: The social side of bacterial stress responses. *Nat. Rev. Microbiol.* **2013**, *11*, 285–293. [[CrossRef](#)]
12. Bruger, E.L.; Snyder, D.J.; Cooper, V.S.; Waters, C.M. Quorum sensing provides a molecular mechanism for evolution to tune and maintain investment in cooperation. *ISME J.* **2021**, *15*, 1236–1247. [[CrossRef](#)] [[PubMed](#)]
13. Bruger, E.L.; Waters, C.M. Maximizing growth yield and dispersal via quorum sensing promotes cooperation in *Vibrio* bacteria. *Appl. Environ. Microbiol.* **2018**, *84*, e00402-18. [[CrossRef](#)] [[PubMed](#)]
14. Bruger, E.L.; Waters, C.M. Bacterial quorum sensing stabilizes cooperation by optimizing growth strategies. *Appl. Environ. Microbiol.* **2016**, *82*, 6498–6506. [[CrossRef](#)] [[PubMed](#)]
15. Dandekar, A.A.; Chugani, S.; Greenberg, E.P. Bacterial quorum sensing and metabolic incentives to cooperate. *Science* **2012**, *338*, 264–266. [[CrossRef](#)] [[PubMed](#)]
16. Hibbing, M.E.; Fuqua, C.; Parsek, M.R.; Peterson, S.B. Bacterial competition: Surviving and thriving in the microbial jungle. *Nat. Rev. Microbiol.* **2010**, *8*, 15–25. [[CrossRef](#)] [[PubMed](#)]
17. Griffin, A.S.; West, S.A.; Buckling, A. Cooperation and competition in pathogenic bacteria. *Nature* **2004**, *430*, 1024–1027. [[CrossRef](#)] [[PubMed](#)]
18. Foster, K.R.; Wenseleers, T. A general model for the evolution of mutualisms. *J. Evol. Biol.* **2006**, *19*, 1283–1293. [[CrossRef](#)] [[PubMed](#)]
19. Stone, L. The stability of mutualism. *Nat. Commun.* **2020**, *11*, 2648. [[CrossRef](#)] [[PubMed](#)]
20. Zhang, Z.; Yan, C.; Zhang, H. Mutualism between antagonists: Its ecological and evolutionary implications. *Integr. Zool.* **2021**, *16*, 84–96. [[CrossRef](#)]
21. Watkins, E.R.; Maiden, M.C.; Gupta, S. Metabolic competition as a driver of bacterial population structure. *Future Microbiol.* **2016**, *11*, 1339–1357. [[CrossRef](#)]
22. Rosenzweig, M.L. Paradox of enrichment: Destabilization of exploitation ecosystems in ecological time. *Science* **1971**, *171*, 385–387. [[CrossRef](#)] [[PubMed](#)]
23. Lempp, M.; Lubrano, P.; Bange, G.; Link, H. Metabolism of non-growing bacteria. *Biol. Chem.* **2020**, *401*, 1479–1485. [[CrossRef](#)] [[PubMed](#)]
24. Alfinito, E.; Cesaria, M.; Beccaria, M. Did Maxwell dream of electrical bacteria? *Biophysica* **2022**, *2*, 281–291. [[CrossRef](#)]
25. Alfinito, E.; Beccaria, M.; Cesaria, M. Cooperation in bioluminescence: Understanding the role of autoinducers by a stochastic random resistor model. *Eur. Phys. J. E* **2023**, *46*, 94. [[CrossRef](#)] [[PubMed](#)]
26. Miller, J.; Parker, M.; Bourret, R.B.; Giddings, M.C. An agent-based model of signal transduction in bacterial chemotaxis. *PLoS ONE* **2010**, *5*, e9454. [[CrossRef](#)]
27. Wang, Y.; Rattray, J.B.; Thomas, S.A.; Gurney, J.; Brown, S.P. In silico bacteria evolve robust cooperation via complex quorum-sensing strategies. *Sci. Rep.* **2020**, *10*, 8628. [[CrossRef](#)]



28. Leaman, E.J.; Geuther, B.Q.; Behkam, B. Hybrid centralized/decentralized control of a network of bacteria-based bio-hybrid microrobots. *J. Micro-Bio Robot.* **2019**, *15*, 1–12. [[CrossRef](#)]
29. Stauffer, D.; Aharony, A. *Introduction to Percolation Theory*, 2nd ed.; CRC Press: Boca-Raton, FL, USA, 2018.
30. Alfinito, E.; Reggiani, L.; Pousset, J. Proteotronics: Electronic devices based on proteins. In *Sensors: Proceedings of the Second National Conference on Sensors, Rome, Italy, 19–21 February 2014*; Springer International Publishing: Cham, Switzerland, 2014; pp. 3–7.
31. Cataldo, R.; Leuzzi, M.; Alfinito, E. Modelling and development of electrical aptasensors: A short review. *Chemosensors* **2018**, *6*, 20. [[CrossRef](#)]
32. Alfinito, E.; Beccaria, M.; Fachechi, A.; Macorini, G. Reactive immunization on complex networks. *Europhys. Lett.* **2017**, *117*, 18002. [[CrossRef](#)]
33. Hill, V. A new mathematical treatment of changes of ionic concentration in muscle and nerve under the action of electric currents, with a theory as to their mode of excitation. *J. Physiol.* **1910**, *40*, 190–224. [[CrossRef](#)]
34. Goutelle, S.; Maurin, M.; Rougier, F.; Barbaut, X.; Bourguignon, L.; Ducher, M.; Maire, P. The Hill equation: A review of its capabilities in pharmacological modelling. *Fundam. Clin. Pharmacol.* **2008**, *22*, 633–648. [[CrossRef](#)] [[PubMed](#)]
35. Dockery, J.D.; Keener, J.P. Mathematical model for quorum sensing in *Pseudomonas Aeruginosa*. *Bull. Math. Biol.* **2001**, *63*, 95–116. [[CrossRef](#)] [[PubMed](#)]
36. Ward, J.P.; King, J.R.; Koerber, A.J.; Williams, P.; Croft, J.M.; Sockett, R.E. Mathematical modelling of quorum sensing in bacteria. *IMA J. Math. Med. Biol.* **2001**, *18*, 263–292. [[CrossRef](#)]
37. Frederick, M.R.; Kuttler, C.; Hense, B.A.; Eberl, H.J. A mathematical model of quorum sensing regulated EPS production in biofilm communities. *Theor. Biol. Med. Model.* **2011**, *8*, 8. [[CrossRef](#)] [[PubMed](#)]
38. Goryachev, A.B. Understanding Bacterial Cell-Cell Communication with Computational Modeling. *Chem. Rev.* **2011**, *111*, 238–250.
39. Sinclair, P.; Brackley, C.A.; Carballo-Pacheco, M.; Allen, R.J. Model for quorum-sensing mediated stochastic biofilm nucleation. *Phys. Rev. Lett.* **2022**, *129*, 198102. [[CrossRef](#)]
40. Ben-Jacob, E.; Schochet, O.; Tenenbaum, A.; Cohen, I.; Czirok, A.; Vicsek, T. Generic modelling of cooperative growth patterns in bacterial colonies. *Nature* **1994**, *368*, 46–49.
41. Pérez-Velázquez, J.; Gölgeli, M.; García-Contreras, R. Mathematical modelling of bacterial quorum sensing: A review. *Bull. Math. Biol.* **2016**, *78*, 1585–1639. [[CrossRef](#)]

**Disclaimer/Publisher’s Note:** The statements, opinions and data contained in all publications are solely those of the individual author(s) and contributor(s) and not of MDPI and/or the editor(s). MDPI and/or the editor(s) disclaim responsibility for any injury to people or property resulting from any ideas, methods, instructions or products referred to in the content.